Tectonophysics 592 (2013) 39–45

Contents lists available at SciVerse ScienceDirect

Tectonophysics

journal homepage: www.elsevier.com/locate/tecto

GPS constraints on continental deformation in the Armenian region and Lesser Caucasus

A. Karakhanyan [a], P. Vernant [b,*], E. Doerflinger [b], A. Avagyan [a], H. Philip [b], R. Aslanyan [c], C. Champollion [b], S. Arakelyan [c], P. Collard [b], H. Baghdasaryan [a], M. Peyret [b], V. Davtyan [a], E. Calais [d], F. Masson [e]

[a] Institute of Geological Sciences, Armenian Academia of Sciences, 24 Baghramian ave, Yerevan, Armenia
[b] Lab. Geosiences Montpellier, University Montpellier 2-CNRS, 34095 Montpellier, France
[c] GEORISK Scientific Research Company, 24a Baghramian Avenue, Yerevan 375019, Armenia
[d] Department of Earth and Atmospheric Sciences, Purdue University, West Lafayette, IN 47906, USA
[e] Institut de Physique du Globe de Strasbourg-UMR7516, Université de Strasbourg/EOST, CNRS, 67084 Strasbourg, France

ARTICLE INFO

Article history:
Received 7 August 2012
Received in revised form 31 January 2013
Accepted 3 February 2013
Available online 12 February 2013

Keywords:
Active tectonics
GPS
Geodynamics
Earthquakes

ABSTRACT

We present the 1998–2009 GPS-derived velocity field for the Armenia region based on a survey-mode observation network of 31 GPS sites. We combine our results with previous GPS studies of the region to better assess the deformation of the Lesser Caucasus and Kura basin region. The results show that the Kura basin and the Lesser Caucasus regions are two different blocks, and that the main fault (Pambak–Sevan–Sunik) between these two regions has a right-lateral slip rate of 2 ± 1 mm/yr. This is consistent with morphotectonic estimates and suggests a fairly constant slip rate over the last 120–300 ka. The right-lateral slip rate on one of the southern branch of the Pambak–Sevan–Sunik fault is lower than 1 mm/yr and the good agreement with a geologically estimated slip rate suggests a constant slip rate over the last 1.4 Myr. The Sardarapat and Akhurian faults experience some shortening. This shortening is consistent with some independent geological estimates and shows the Arabian push. However, NNW-SSE-orientated faults have an extensional fault normal component instead of the expected shortening due to the Arabia–Eurasia convergence. This substantial extensive strain, and the sharp azimuth change of the velocity vectors between the Arabia promontory and the Lesser Caucasus suggest that processes other than "extrusion", possibly related to old subduction or delamination, contribute to the geodynamics of the region.

1. Introduction

Armenia and the neighboring areas of Azerbaijan, Georgia and Eastern Turkey are located in the central part of the Arabia–Eurasia collision zone. This region results from the accretion of continental fragments to the southern Eurasian margin by the late Cretaceous to early Tertiary (e.g., Sengör, 1990). Arabia is moving northward relative to Eurasia at a rate of approximately 17 mm/yr based on GPS estimates (Reilinger et al., 2006; Vernant et al., 2004). This rate of convergence seems to have been fairly constant since the onset of the intra-continental tectonics about 12 Ma ago (e.g., McQuarrie et al., 2003). Volcanic activity has been ongoing since 6–8 Ma (Innocenti et al., 1976; Pearce et al., 1990). Focal mechanisms, slip vectors and GPS velocities point out a spatial separation between thrusts and strike-slip faults (e.g., Jackson, 1992; Reilinger et al., 2006). The Caucasus accommodates NE-SW shortening perpendicular to the strike of the belt while the remainder of the convergence is taken up on strike-slip faults in the Armenian Highlands (also referred Turkish–Iranian plateau) and the Lesser Caucasus (Fig. 1). Numerical modeling studies (Vernant and Chery, 2006) suggest that Arabia–Eurasia collision induced forces alone cannot explain the present-day velocity field, and that other forces (such as for example a slab pull beneath the Caucasus) are needed to explain the kinematic of the region.

This paper is concerned with active faulting in the Lesser Caucasus which accommodates a part of the Arabia–Eurasia convergence. The Lesser Caucasus experiences N-S shortening and E-W extension, accompanied with faulting and earthquakes (Copley and Jackson, 2006; Dewey et al., 1986; Jackson, 1992; Jackson and McKenzie, 1984; Taymaz et al., 1991). The faults in the Lesser Caucasus region are generally short strike-slip faults with either a reverse-slip or normal-slip components (Karakhanian et al., 2004). However, these faults, with a maximum length of 350–450 km, can generate earthquakes with magnitude up to $M = 7.5$ (Ambraseys and Melville, 1982; Berberian, 1997; Karakhanyan and Abgaryan, 2004). With a complex seismic activity and low present-day deformation rates the geodynamics of this area is still poorly understood. The assessments of fault slip rates, potential magnitudes and recurrence intervals of earthquakes are still fragmentary and ambiguous.

Present-day deformation rates in Armenia have been measured using survey mode GPS since 1991 (McClusky et al., 2000; Reilinger, 1998; Reilinger et al., 1997, 2006), and the Yerevan continuous GPS station has been operating from 1996 up to 2010. However, the velocity field is still sparse and Reilinger et al. (2006) have suggested that

* Corresponding author. Tel.: +33 467144892.
E-mail address: pvernant@um2.fr (P. Vernant).

0040-1951/$ – see front matter © 2013 Elsevier B.V. All rights reserved.
http://dx.doi.org/10.1016/j.tecto.2013.02.002

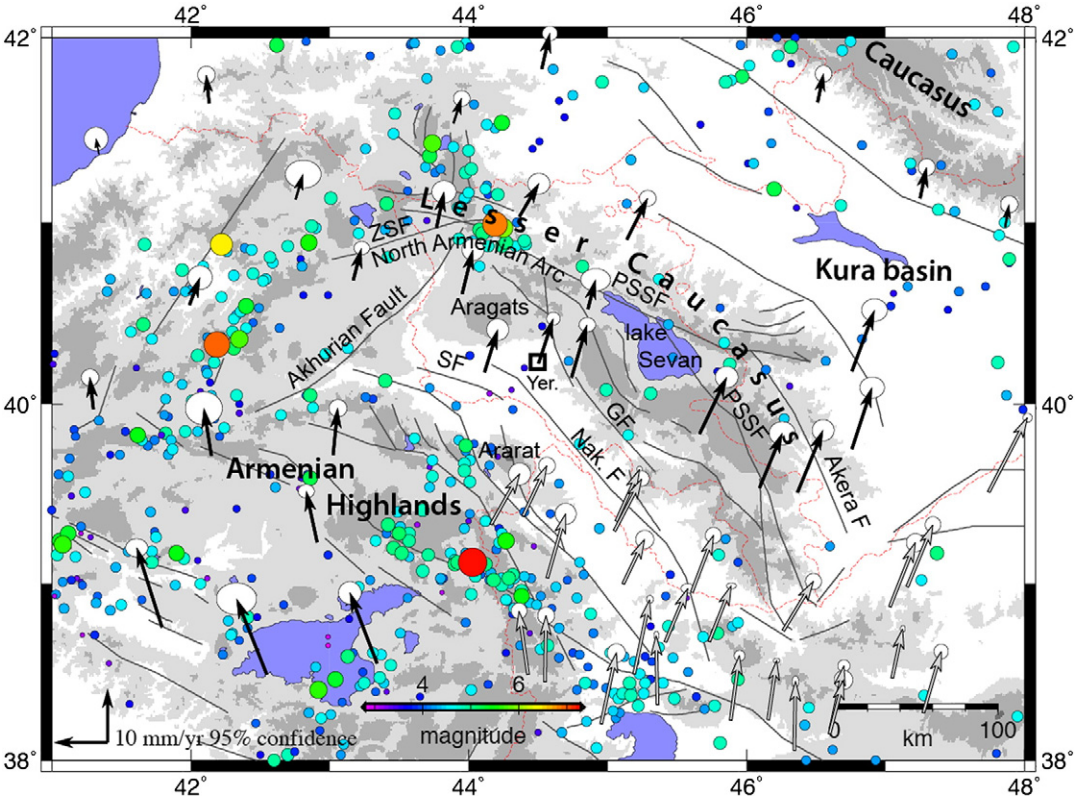

Fig. 1. Summary structural map adapted from Jackson et al. (2002), Karakhanian et al. (2004) and Copley and Jackson (2006). Seismicity is from National Earthquake Information Center catalog (neic.usgs.gov) of crustal earthquakes with magnitudes from 3 to 6.5 (1976–2011). Black GPS vectors are from Reilinger et al. (2006) and gray GPS vectors are from Djamour et al. (2011). Both GPS velocity fields are relative to fixed Eurasia. GF, Garni fault; PSSF, Pambak–Sevan–Sunik fault; SF, Sardarapat fault; ZSF, Zheltorechensk–Sarighamish fault; Yer., Yerevan.

deformation across the Lesser Caucasus was not significant given the uncertainties they had on the present-day velocities.

Since 1998, the Institute of Geological Sciences of the National Academy of Sciences (Armenia), Montpellier-2 University (France) and GEORISK Scientific Research CJS (Armenia) have conducted GPS surveys across Armenia. A GPS network of 31 sites was installed in the central and northern parts of Armenia. In this work, we present the results of 4 surveys conducted during the period from 1998 to 2009. The network encompasses the central part of the North-Armenian Arc cut by several active strike-slip faults whose major ones are: Pambak–Sevan–Sunik fault (PSSF), Garni fault (GF), Zheltorechensk–Sarighamish fault (ZSF), Akhurian fault (AhF), Sardarapat fault (SF) and Akera fault (Fig. 1). The North-Armenian Arc if formed by left-lateral strike-slip faults (ZSF and AhF) and right-lateral strike-slip faults (PSSF and GF) that merge together north of the Aragats volcano (Karakhanian et al., 2004). This area is the place where the Spitak earthquake occurred in 1988 ($M_W = 6.9$, Karakhanian et al., 2004; Philip et al., 1992; Trifonov et al., 1994), killing more than 25,000 people. South of the North Armenian Arc, the triangular shaped region delimited by the Akhurian Fault to the west and Garni fault to the east, is the region where the largest Armenian strato-volcano is located (Mount Aragats). This is also the region where the Yerevan city is located (1.5 million people), as well as the Armenian Nuclear Power Plant. The region located between the GF and the PSSF shows intense Holocene–Quaternary volcanism along a NNW-SSE linear trend and the volcano-tectonic depression of the lake Sevan. During the historical period, the segments of GF and PSSF bordering this region have produced earthquakes with $M = 7.0–7.5$ accompanied with volcanic eruptions (Karakhanian et al., 2004).

In this paper we use GPS velocities from 31 new survey mode sites to estimate the slip rate of the main Lesser Caucasus active faults and to discuss the geodynamics of the region.

2. GPS data and analysis

The observed GPS network covers an area of 180 km E-W by 150 km N-S wide. The measurements were made using dual-frequency geodetic GPS Ashtech Z12 and Ashtech ZX receivers, equipped with Chock Ring-type Ashtech antennas. We use 31 survey sites installed with an average spacing of the order of 20 km. The sites BAV0, BUR0, CHO0, ERA0, GEG0, KIZ0, MET0, SA10, and SA20 have been surveyed in 1998, 2000, 2003, and 2009. The sites AKH0, ENO0, KAR0, ODZ0, PAM0, RAZ0, SHA0, SUB0, TSA0, ZOD0, and ZOL0 have been surveyed in 1998, 2000 and 2003. The site KHO0 has been surveyed in 1998 and 2000. All the site ending in "0" were surveyed using tripod setups and could therefore potentially be subject to setup centering errors of ± 2 mm. The effect of these centering errors on the estimated velocities are evaluated and discussed later in this section. The sites ARA4, BAV4, BUR4, CHO4, ERA4, GEG4, KIZ4, MET4, SA14, and SA24 have been surveyed in 2003 and 2009, using a constrained centering technique, in which the antenna is screwed directly to the survey monument ensuring near exact centering at each survey. Each site has been measured for at least 48 h during each session.

We use the GAMIT/GLOBK software package (Herring et al., 2009a,b,c) to compute the coordinates and velocities of the 31 survey GPS sites using a three-step strategy (Dong et al., 1998; Feigl et al., 1993). GPS data of 14 IGS stations were introduced in the process to tie our local network to the ITRF reference frame. Our local quasi-observations were combined with

the global quasi-observations provided by MIT (http://www-gpsg.mit.edu/~simon/gtgk/index.htm) from 1996 to 2009. Following Reilinger et al. (2006), we use the "real sigma" algorithm they describe to account for the correlated errors in the time series by calculating a unique noise model for each continuous GPS station. Since our Armenian sites are only measured episodically using the survey setup approach, we cannot use the "real sigma" technique above, as it is only applicable to continuous time series data. Instead, we use the correlated noise model values determined by Djamour et al. (2011) for the CGPS in NW Iran. Following Djamour et al. (2011), we applied a 0.95 mm/√yr random walk stochastic noise to the SGPS horizontal time series estimates. For the vertical random walk noise value we use 3 mm/√yr. These values are also consistent with the values estimated by Djamour et al. (2010) for the Alborz range. Velocities and there 1sig confidence uncertainties were estimated in the ITRF2008 reference frame and then transformed into the Eurasian reference frame by minimizing the horizontal velocities of 23 IGS stations located in Europe and Central Asia (ARTU, BOR1, BRUS, GRAS, GRAZ, IRKT, JOZE, KOSG, KSTU, MADR, METS, NYAL, ONSA, POTS, TIXI, TOUL, TROM, VILL, WTZR, YAKT, ZECK, ZIMM, ZWEN). The wrms value for the velocity residuals of these 23 sites is 0.1 mm/yr. Our data have been combined with the daily solutions of Djamour et al. (2011) to ensure the best combination, we have 10 to 15 sites in common. We then plot this combined velocity field together with the solution from Reilinger et al. (2006) (Fig. 2). Our Armenian velocities are given in Table 1 in a Eurasia-fixed reference frame. The sites having the same three first letters are collocated; those ending with 0 have been surveyed with tripods, the others being forced centering. All the velocities of these collocated sites are within the uncertainties and show that there was minimal bias introduced by the tripod setup measurements. Except for the continuous station NSSP, no Armenian sites from Reilinger et al. (2006) solution are common with ours. For the three sites common between Reilinger et al. (2006) solution and our combined own solution and Djamour et al. (2011) one, the RMS is 0.69 mm/yr, within the average 2σ velocity uncertainty. Our velocities show the expected NNE direction with an increase in velocities from west to east. No large change occurs across the main faults as already suggested by Reilinger et al. (2006). Using a block-like approach, we propose to see if we can quantify the main fault slip rates.

3. Block model kinematics analysis and fault slip rate estimates

Our goal is to estimate the fault slip rates on the main Armenian active faults, we will use a block model approach (McCaffrey, 2002) to do so. However, it should be noted that our block model does not mean that no deformation occurs within the blocks. Several historical earthquakes have been reported within the blocks derived from velocity fields (e.g. Allen et al., 2011; Karakhanian et al., 2004; Le Dortz et al., 2009) and instrumental seismicity occurs from time to time within a block (Fig. 1). Reilinger et al. (2006) suggest that no significant deformation occurs within the Lesser Caucasus and Kura region, however they note that splitting this broad region into two blocks (the Lesser Caucasus block and the Kura block) leads to fault slip rate estimates that are in agreement with geological estimates. In order to check if our denser network allows for a better quantification of the fault slip rates in Armenia and the Lesser Caucasus, we develop a block model based on the main mapped active faults in the region. No significant earthquake occurred during the time interval of the measurements, and no postseismic transients are expected in this region. Hence our GPS measurements are supposed to depict the inter-seismic deformation of Armenia. Given the very low slip rates expected in the region and the rather small size of the blocks, one can only expect for a very low elastic transient. Indeed, the highest reported fault slip rate in the region based on dated offset markers is about 2.24 ± 0.96 mm/yr (Philip et al., 2001). Based on the elastic dislocation theory, the change from the rigid part of the block to the fault will be half of the fault slip rate (Savage and Burford, 1973), which in our case means less than 1 mm/yr. Given that our 95% confidence uncertainties are on the order of 1 mm/yr, trying to solve for the interseismic deformation and the locking

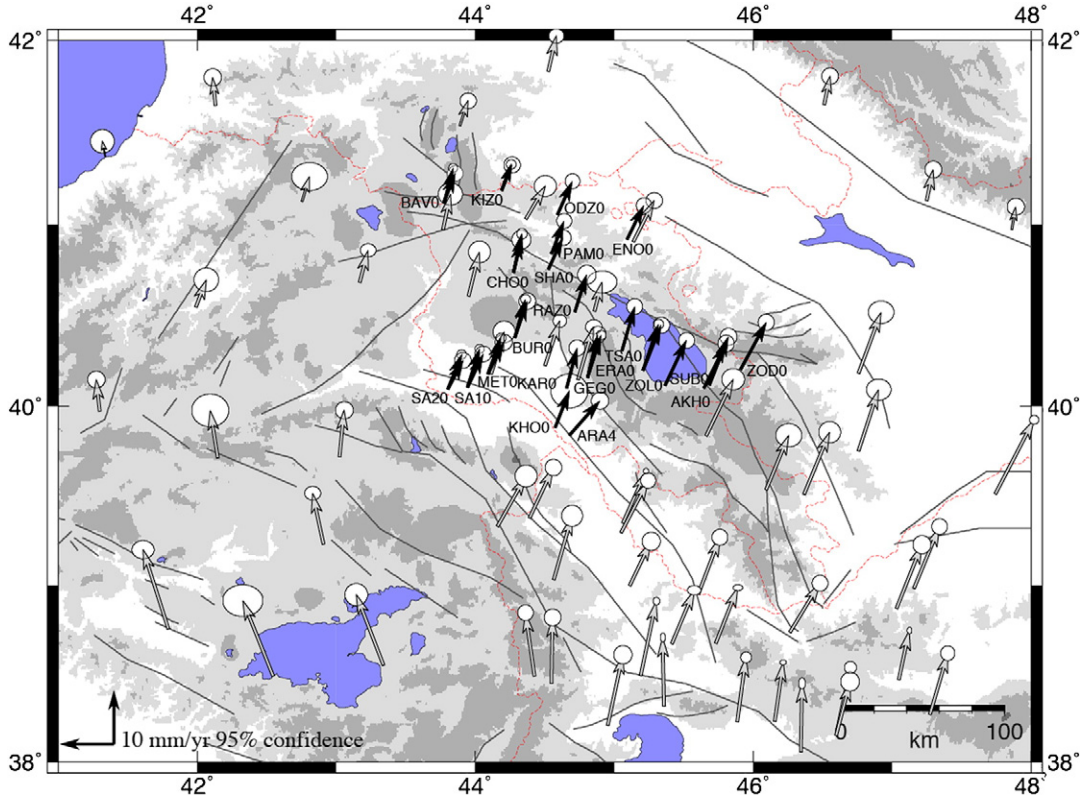

Fig. 2. Map showing GPS velocities and 95% confidence ellipses relative to Eurasia determined in this study (black vectors, all velocities are given in Table 1) and gray vectors are from Reilinger et al. (2006) and Djamour et al. (2011).

Table 1
East and north GPS velocity components (E Vel., N Vel.) and 1σ uncertainties (σ E, σ N) in a Eurasia-fixed reference frame as determined in this study are given in mm/yr. ρEN is the correlation between E and N velocities. An "*" in the site column designates continuous GPS stations.

Longitude, °E	Latitude, °N	E Vel., mm/yr	N Vel., mm/yr	σ E, mm/yr	σ N, mm/yr	ρEN	Site name
45.645	40.099	4.1	8.3	0.6	0.6	0.004	AKH0
44.679	39.840	5.7	6.4	0.6	0.6	0.000	ARA4
43.782	41.121	1.7	6.5	0.3	0.3	0.000	BAV0
43.782	41.121	2.1	5.4	0.6	0.6	0.000	BAV4
44.287	40.381	2.0	7.0	0.4	0.4	−0.012	BUR0
44.287	40.381	2.3	6.7	0.6	0.6	−0.017	BUR4
44.276	40.736	1.6	7.3	0.4	0.4	−0.006	CHO0
44.276	40.736	1.5	6.2	0.7	0.7	−0.011	CHO4
45.094	40.920	3.1	6.3	0.6	0.6	−0.006	ENO0
45.209	40.198	2.9	8.6	0.4	0.4	0.002	ERA0
45.209	40.198	3.4	8.4	0.6	0.6	0.005	ERA4
44.810	40.160	2.5	7.8	0.4	0.4	−0.007	GEG0
44.810	40.159	1.9	8.0	0.6	0.6	−0.008	GEG4
44.657	40.101	2.0	7.4	0.6	0.6	−0.003	KAR0
44.575	39.881	2.7	6.8	1.4	1.3	0.044	KHO0
44.190	41.185	1.8	4.9	0.4	0.4	−0.006	KIZ0
44.190	41.185	1.9	4.7	0.6	0.6	−0.015	KIZ4
44.091	40.178	2.4	6.7	0.4	0.4	−0.011	MET0
44.091	40.178	2.9	5.9	0.6	0.6	−0.016	MET4
44.503	40.226	2.2	7.2	0.1	0.1	−0.013	NSSP*
44.593	41.055	2.8	6.2	0.6	0.6	−0.004	ODZ0
44.550	40.840	2.4	6.1	0.6	0.6	−0.006	PAM0
44.718	40.520	2.2	6.9	0.7	0.7	−0.006	RAZ0
43.951	40.108	2.3	7.2	0.4	0.3	0.000	SA10
43.951	40.108	2.9	6.2	0.6	0.6	0.000	SA14
43.807	40.097	2.6	6.5	0.4	0.4	−0.002	SA20
43.807	40.097	2.8	5.4	0.6	0.6	−0.001	SA24
44.528	40.753	2.7	5.9	0.6	0.6	−0.003	SHA0
45.686	40.117	3.5	9.0	0.6	0.7	−0.007	SUB0
45.055	40.307	2.4	8.2	0.6	0.6	−0.004	TSA0
45.908	40.204	4.8	8.7	0.6	0.6	−0.002	ZOD0
45.367	40.114	4.0	8.4	0.6	0.6	0.004	ZOL0
58.560	56.430	−0.25	0.13	0.11	0.13	−0.017	ARTU*
17.073	52.277	−0.03	0.11	0.14	0.09	−0.011	BOR1*
4.359	50.798	−0.10	−0.84	0.17	0.14	−0.004	BRUS*
6.921	43.755	0.17	0.16	0.11	0.10	−0.010	GRAS*
15.493	47.067	0.79	0.67	0.16	0.21	−0.005	GRAZ*
104.316	52.219	−0.32	−0.79	0.19	0.19	0.000	IRKT*
21.032	52.097	0.02	0.28	0.12	0.09	−0.017	JOZE*
5.810	52.178	0.04	0.68	0.13	0.11	−0.006	KOSG*
92.794	55.993	−0.97	−1.31	0.22	0.22	0.001	KSTU*
355.750	40.429	−0.48	−0.25	0.18	0.16	−0.001	MADR*
24.395	60.217	0.20	−0.84	0.10	0.09	−0.018	METS*
11.865	78.930	−0.24	−0.94	0.11	0.10	−0.004	NYAL*
11.926	57.395	−0.81	−0.54	0.09	0.10	−0.011	ONSA*
13.066	52.379	−0.33	0.06	0.26	0.26	−0.003	POTS*
128.866	71.634	0.14	0.09	0.15	0.19	0.008	TIXI*
1.481	43.561	−0.48	0.80	0.50	0.50	−0.001	TOUL*
18.938	69.663	−0.69	0.95	0.11	0.10	−0.011	TROM*
356.048	40.444	−0.13	0.13	0.13	0.09	−0.005	VILL*
12.879	49.144	−0.02	0.18	0.10	0.09	−0.014	WTZR*
129.680	62.031	−0.14	−0.84	0.42	0.33	0.003	YAKT*
41.565	43.788	−0.44	0.76	0.16	0.10	−0.013	ZECK*
7.465	46.877	0.55	0.44	0.11	0.09	−0.011	ZIMM*
36.759	55.699	0.35	0.33	0.13	0.14	−0.011	ZWEN*

depth on the faults is pointless in this case. Therefore we only solve for the rigid rotation of each block by minimizing the residuals between the observed velocities and the modeled velocities using a plate like motion of each block (Euler vectors are given in Table 2).

Following Reilinger et al. (2006), we first develop a model with single block combining the Kura basin and the Lesser Caucasus region. In this case the wrms is 1.09 mm/yr and less than 58% of the 62 sites have residuals lower than the 95% uncertainties. Reilinger et al. (2006) pointed out that splitting this block in two with the Pambak–Sevan–Sunik fault was not significant. In order to check if our data significantly improve our understanding of the region, we have developed a simpler block model using only two blocks: the Lesser Caucasus and the Kura (Fig. 3). The wrms obtained is 0.92 mm/yr, which is less than for the previous model with only one block. The fit to the GPS data is better than the previous model; ten sites on the Ararat block, two sites on the Aragats block, four sites on the Gegharkunik block and one site that was on the Eastern Lesser Caucasus block have residuals higher than their 95% uncertainties. Hence, 68% of the 62 sites have residuals lower than their 95% uncertainties. As suggested by Stein and Gordon (1984), we use an F-ratio test to check if the improvement in fit of the model to the data resulting from the addition of another block to the model is greater than that expected purely by chance. The F-ratio test confirms that the better fit is significant with $F = 15.3$ being much greater than the value of $F_{0.01} \sim 3.95$, for $\nu_1 = 3$, $\nu_2 = 118$. Hence, to the contrary of Reilinger et al. (2006) we are able to estimate a significant slip rate for the Pambak–Sevan–Sunik. This model gives a right-lateral slip rate for the Pambak–Sevan–Sunik fault of ~2.1 mm/yr (Fig. 3). This value is consistent with the estimate of 2.24 ± 0.96 mm/yr (Philip et al., 2001). The fault normal component of the PSSF shows a very low shortening for the NW segments, and a high extension for the SE segments. The residuals within the Lesser Caucasus block are small and suggest that the slip rates on the other Armenian faults (Garni, Zheltorechensk–Sarighamish, Akhurian, and Sardarapat) must be very low. The residuals higher than the uncertainties south of the Lesser Caucasus block suggest that some shortening take place in this region.

To quantify the slip rates of the other Armenian faults and see if we are able to decipher any internal deformation of the Lesser Caucasus block, we develop a model based on the main active faults of the region. The geometry of the model is shown on Fig. 4. Using the Pambak–Sevan–Sunik fault (PSSF), Garni fault (GF), Akhurian fault (AhF), the Sardarapat fault (SF) and the Akera fault (Fig. 1), we decompose the Lesser Caucasus into five blocks: the Kars block, the Aragats block, the Ararat block, the Gegharkunik block and the Eastern Lesser Caucasus block (Fig. 4). The weighed root mean square (wrms) estimated for the Lesser Caucasus and Kura region is 0.82 mm/yr. Only three of the 15 sites on the Kura block have a residual higher than the 95% uncertainty (Fig. 4). All the residuals of the Kars (4 sites) and Eastern Lesser Caucasus (3 sites) blocks are within the 95% uncertainties. One site of the Aragats block (12 sites) has a residual velocity higher than its uncertainty. Seven sites of the Ararat block (15 sites), and three sites of the Gegharkunik block (13 sites) have residual velocities higher than their 95% uncertainties. This means that more than 77% of the 62 sites of the Lesser Caucasus–Kura region are within the 95% uncertainties.

With a value $F = 2.19$ being smaller than the value of $F_{0.01} \sim 2.36$, but larger than $F_{0.02} \sim 2.14$, for $\nu_1 = 12$, $\nu_2 = 106$, there is less than 2% chance that the improvement in fit is due purely to chance. The central segment of the Pambak–Sevan–Sunik fault has an estimated right lateral slip rate of 2.24 ± 0.96 mm/yr (Philip et al., 2001, Fig. 5). Our estimated slip rate is 2 mm/yr, suggesting a constant slip rate over the last 120–300 ka. Furthermore this right lateral slip rate is the same as the one previously estimated with the 2-block model. For the other fault segments, the computed slip rates are lower than 1 mm/yr (Fig. 5). Given that the improvement of this model relative to the 2-block model is only marginal, the slip rates obtained for the faults bounding the Lesser Caucasus blocks should be used with caution, keeping in mind that the uncertainty on the slip rate is of ~0.8 mm/yr. As an independent way of estimating the uncertainties, we discuss the consistency of our estimates slip rates with the geological rates. The right lateral slip rate obtained for the Pambak–Sevan–Sunik segment bounding the Eastern Lesser Caucasus block to the west (0.3 mm/yr, Fig. 5) is consistent with the geological slip rate of 0.53 ± 0.04 mm/yr based on the offset of a volcanic cone (Philip et al., 2001), but is significantly lower than the 4–5 mm/yr estimated by Trifonov et al. (Trifonov et al., 1994). Trifonov et al. (1994) provide a right lateral slip rate estimate on the northern Garni fault segment of 3 ± 0.5 mm/yr (Fig. 5). Our study suggests a right lateral slip rate with a lower value of 0.6 mm/yr.

Table 2
Euler vectors relative to Eurasia and 1 s uncertainties for the block model determined in this study. The wrms are for the model with 5 sub-Lesser Caucasus block.

Blocks, plates	Longitude, °E	σ	Latitude, °N	σ	Rate, °/Myr	σ	Corr. lat/lon	Corr. lat/rate	Corr. lon/rate	wrms, mm/yr	Number of sites
Kura-EU	40.507	0.54	42.199	0.19	1.067	0.107	−0.654	−0.694	0.942	0.78	15
Kars-EU	36.843	4.66	41.944	0.82	0.634	0.475	−0.862	−0.868	0.993	0.28	4
Aragats-EU	39.444	2.50	41.341	0.47	1.040	0.523	−0.951	−0.953	0.997	0.49	12
Ararat-EU	36.346	2.16	41.839	0.55	0.710	0.180	−0.934	−0.941	0.993	1.01	15
Geghar-EU	40.301	1.11	41.389	0.29	1.158	0.255	−0.894	−0.904	0.989	0.78	13
ELCB-EU	39.923	4.42	41.799	1.23	1.111	0.784	−0.973	−0.976	0.997	0.79	3

Given the length of the segments of the Pambak–Sevan–Sunik fault (90–120 km, Karakhanian et al., 2004), using an average depth for the fault rupture of 15 km, the recurrence time for earthquakes similar to the largest historical earthquake reported (M 7.5–7.7, 1139, Karakhanian et al., 2004) is about 2000–4000 yr. Recurrence time for M ~7 earthquakes on the PSSF is about 500 yr. For the Garni fault, recurrence times for M ~7 and M ~7.3 earthquakes are 3000 and 8000 yr respectively.

The fault normal shortening (or extension) components are usually small (<1 mm/yr) and suggest extension along the Garni and PSSF fault west of the Eastern Lesser Caucasus block (Fig. 5). This is consistent with the recent volcanic activity that occurred along these faults (Karakhanian et al., 2004). Compression occurs on the Sardarapat and southern Akhurian faults with value of fault normal component of ~1 mm/yr. This compression is consistent with the uplift observed with archeological data along the Sardarapat fault (Karakhanian et al., 2004). The deduced uplift is ~0.7 mm/yr, which depending on the isostatic compensation related to the fault activity suggests a fault dip ranging from 30 to 75°. More importantly, this compression evidences the Arabian push in the Lesser Caucasus region. However, faults orientated roughly NNW-SSE (Garni, eastern Pambak–Sevan–Sunik and Akera faults) have an extensional component. Given the direction of the Arabia–Eurasia convergence, one would expect to have a shortening component on theses faults. This extensional component and the NNW azimuth of the velocities in the Eurasia reference frame suggest that the Arabian push is not the only force acting in the geodynamics of the region and that some pull to the NNW is required. This could be a slab pull effect beneath the Caucasus as suggested previously (Djamour et al., 2011; Masson et al., 2006; Vernant and Chery, 2006) possibly combined to some delamination beneath the Lesser Caucasus (Sosson et al., 2010).

4. Conclusion

Even though strain rates are small within the region of the Lesser Caucasus, our GPS measurements in Armenia, which sometimes cover a time span of 11 yr, allow us to go more into the details of the deformation of the region than the previous studies (Djamour et al., 2011; McClusky et al., 2000; Reilinger et al., 2006; Vernant et al., 2004). Indeed, Reilinger et al. (2006), based on GPS measurements, suggested

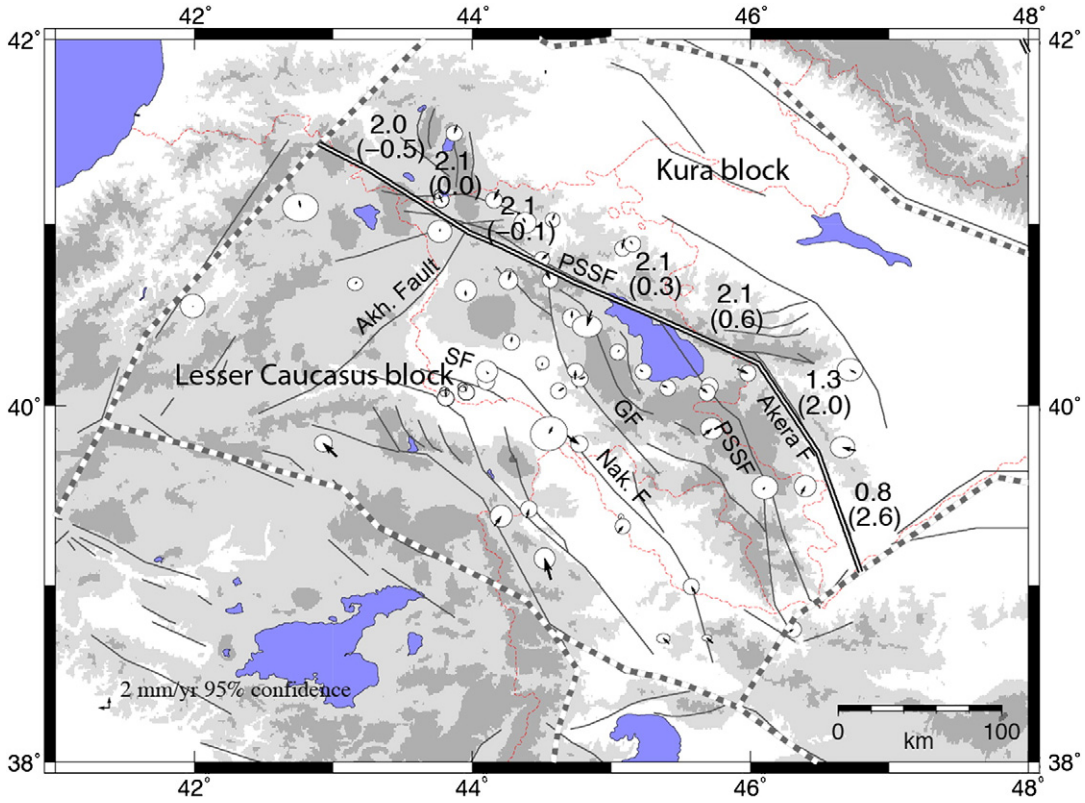

Fig. 3. Map showing block model geometry, residual velocities (observed minus modeled) and 95% confidence ellipses for our model with only one Lesser Caucasus block (see description in the text). Top numbers (no parentheses) are strike-slip rates deduced from this block model geometry, positive being right-lateral. Numbers in parentheses are fault-normal components, negative being closing. Light lines show block boundaries with estimated slip rates, dashed lines show block boundaries with no estimation of slip rates. Akh, Akhurian fault; GF, Garni fault; PSSF, Pambak–Sevan–Sunik fault; SF, Sardarapat fault.

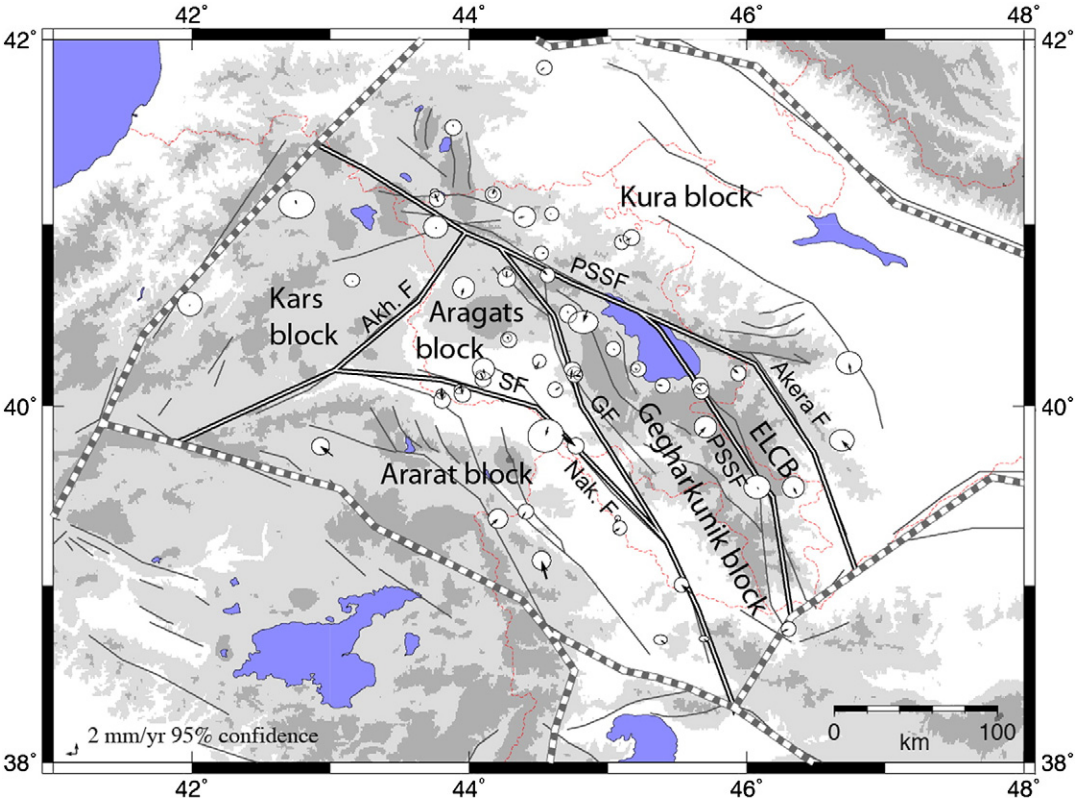

Fig. 4. Map showing block model geometry, residual velocities (observed minus modeled) and 95% confidence ellipses for our model based on the main active faults mapped in Armenia (see description in the text). ELCB, Eastern Lesser Caucasus Block. Light lines show block boundaries with estimated slip rates, dashed lines show block boundaries with no estimation of slip rates. Akh, Akhurian fault; GF, Garni fault; PSSF, Pambak–Sevan–Sunik fault; SF, Sardarapat fault.

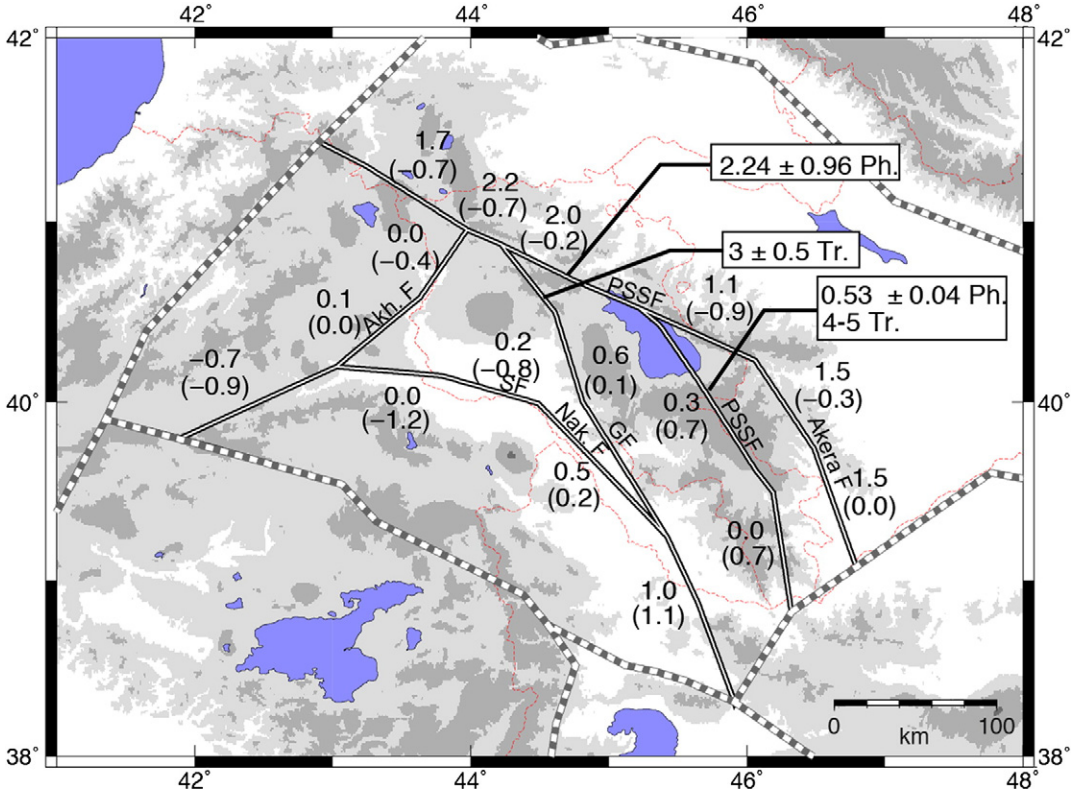

Fig. 5. Map showing fault slip rates (mm/yr) deduced from the block model shown in Fig. 3. Top numbers (no parentheses) are strike-slip rates, positive being right lateral. Numbers in parentheses are fault-normal components, negative being closing. Light lines show block boundaries with estimated slip rates, dashed lines show block boundaries with no estimation of slip rates. Geological slip rate estimates are given in boxes (Ph.: Philip et al., 2001; Tr.: Trifonov et al., 1994). Akh, Akhurian fault; GF, Garni fault; PSSF, Pambak–Sevan–Sunik fault; SF, Sardarapat fault.

that the Kura and the Lesser Caucasus might be two independent blocks, but their relative motion not significant. With our results, it is clear that they are two independent blocks and that the main fault between them must be the Pambak–Sevan–Sunik fault with a geodetic slip rate (2 ± 0.8 mm/yr) in agreement with the geologic slip rate (2.24 ± 0.96 mm/yr, Philip et al., 2001), suggesting a constant slip rate over the last 120–300 ka. Using the main active mapped faults leads to split up the Lesser Caucasus into 5 blocks. The results suggest low fault slip rates that are below the uncertainties, however they are consistent with the geologic slip rate of 0.53 ± 0.04 mm/yr (Philip et al., 2001) and suggest also a fairly constant right lateral slip rate (~2 mm/yr) of the Pambak–Sevan–Sunik fault over the last 1.4 Myr. They also suggest that the main active eastern prolongation of the PSSF is the Akera fault. N-S shortening occurs south of Armenia in agreement with the geological evidences on the Sardarapat fault. This reflects the Arabia–Eurasia collision, however, the fault-orientated NNW-SSE have an extensional fault normal component. This extension is not consistent with the direction of convergence between Arabia and Eurasia, suggesting that some other forces are involved in the geodynamics of the region. They could be related to some remnant subduction beneath the Caucasus as previously suggested (Vernant and Chery, 2006).

Acknowledgments

We thank all the teams who went out in the field to collect the data, and those international colleagues who contribute data to the IGS Tracking network. We thank J.-F. Ritz for the fruitful discussions about the active tectonics of the region and R. Reilinger and an anonymous reviewer for helping us to improve this manuscript. This work was realized in the frame of a cooperative research agreement between INSU-CNRS, MAE (French Foreign Office Ministry) and Georisk (Armenia).

References

Allen, M.B., Kheirkhah, M., Emami, M.H., Jones, S.J., 2011. Right-lateral shear across Iran and kinematic change in the Arabia–Eurasia collision zone. Geophysical Journal International 184 (2), 555–574.

Ambraseys, N.N., Melville, C.P., 1982. A History of Persian Earthquakes. Cambridge University Press, New York (219 pp.).

Berberian, M., 1997. Seismic sources of the Transcaucasian historical earthquakes. In: Giardini, D., Balassanian, S. (Eds.), Historical and Prehistorical Earthquakes in the Caucasus. Kluwer Academic Publishing, Dordrecht, Netherlands, pp. 233–311.

Copley, A., Jackson, J., 2006. Active tectonics of the Turkish–Iranian Plateau. Tectonics 25 (6).

Dewey, J.F., Hempton, M.R., Kidd, W.S.F., Saroglu, F., Sengor, A.M.C., 1986. Shortening of continental lithosphere: the neotectonics of Eastern Anatolia—a young collision zone. In: Coward, M.P., Riea, A.C. (Eds.), Collision Tectonics: Geol. Soc. Lond. pp. 3–36.

Djamour, Y., Vernant, P., Bayer, R., Nankali, H., Ritz, J.F., Hinderer, J., Hatam, Y., Luck, B., Le Moigne, N., Sedighi, M., Khorrami, F., 2010. GPS and gravity constraints on continental deformation in the Alborz mountain range, Iran. Geophysical Journal International 183, 1287–1301. http://dx.doi.org/10.1111/j.1365-246X.2010.04811.

Djamour, Y., Vernant, P., Nankali, H.R., Tavakoli, F., 2011. NW Iran-eastern Turkey present-day kinematics: results from the Iranian permanent GPS network. Earth and Planetary Science Letters 307 (1–2), 27–34.

Dong, D., Herring, T.A., King, R.W., 1998. Estimating regional deformation from a combination of space and terrestrial geodetic data. Journal of Geodesy 72, 200–211.

Feigl, K.L., et al., 1993. Space geodetic measurement of crustal deformation in central and southern California. Journal of Geophysical Research 98, 21677–21712.

Herring, T.A., King, R.W., McClusky, S.C., 2009a. GAMIT Reference Manual, Release 10.3. Massachussetts Institute of Technology, Cambridge.

Herring, T.A., King, R.W., McClusky, S.C., 2009b. GLOBK Reference Manual, Release 10.3. Massachussetts Institute of Technology, Cambridge (91 pp.).

Herring, T.A., King, R.W., McClusky, S.C., 2009c. Introduction to GAMIT/GLOBK, Release 10.35. Massachussetts Institute of Technology, Cambridge (45 pp.).

Innocenti, F., Mazzuoli, R., Pasquare, G., Radicati di Brozolo, F., Villari, L., 1976. Evolution of volcanism in the area of interaction between the Arabian, Anatolian and Iranian plates (Lake Van, Eastern Turkey). Journal of Volcanology and Geothermal Research 1, 103–112.

Jackson, J.A., 1992. Partitioning of strike-slip and convergent motion between Eurasia and Arabia in eastern Turkey and Caucasus. Journal of Geophysical Research 97, 12471–12479.

Jackson, J.A., McKenzie, D.P., 1984. Active tectonics of the Alpine–Himalayan Belt between western Turkey and Pakistan. Geophysical Journal of the Royal Astronomical Society 77, 185–246.

Jackson, J.A., Priestley, K., Allen, M., Berberian, M., 2002. Active tectonics of the South Caspian Basin. Geophysical Journal International 148, 214–245.

Karakhanian, A.S., et al., 2004. Active faulting and natural hazards in Armenia, eastern Turkey and northwestern Iran. Tectonophysics 380 (3–4), 189–219.

Karakhanyan, A., Abgaryan, Y., 2004. Evidence of historical seismicity and volcanism in the Armenian Highland (from Armenian and other sources). Annals of Geophysics 47 (2/3), 793–810.

Le Dortz, K., et al., 2009. Holocene right-slip rate determined by cosmogenic and OSL dating on the Anar fault, Central Iran. Geophysical Journal International 179 (2), 700–710.

Masson, F., et al., 2006. Extension in NW Iran driven by the motion of the south Caspian basin. Earth and Planetary Science Letters 252 (1–2), 180–188.

McCaffrey, R., 2002. Crustal block rotations and plate coupling. In: Stein, S., Freymueller, J.T. (Eds.), Plate Boundary Zones: AGU Geodynamics Series, pp. 101–122.

McClusky, S., et al., 2000. Global positioning system constraints on plate kinematics and dynamics in the eastern Mediterranean and Caucasus. Journal of Geophysical Research, B: Solid Earth and Planets 105 (3), 5695–5719.

McQuarrie, N., Stock, J.M., Verdel, C., Wernicke, B.P., 2003. Cenozoic evolution of Neotethys and implications for the causes of plate motions. Geophysical Research Letters 30 (20). http://dx.doi.org/10.1029/2003GL017992.

Pearce, J.A., et al., 1990. Genesis of collision volcanism in Eastern Anatolia, Turkey. Journal of Volcanology and Geothermal Research 44 (1–2), 189–229.

Philip, H., et al., 1992. The Armenian earthquake of 1988 December 7: faulting and folding, neotectonics and paleoseismicity. Geophysical Journal International 110, 141–158.

Philip, H., Avagyan, A., Karakhanian, A., Ritz, J.-F., Rebai, S., 2001. Estimating slip rates and recurrence intervals for strong earthquakes along an intracontinental fault; example of the Pambak–Sevan–Sunik Fault (Armenia). Tectonophysics 343 (3–4), 205–232.

Reilinger, R. et al., 1998. Velocity field for the eastern Mediterranean. Annales Geophysicae (1988), 16, Suppl. 1: 99.

Reilinger, R.E., et al., 1997. Preliminary estimates of plate convergence in the Caucasus collision zone from Global Positioning System measurements. Geophysical Research Letters 24 (14), 1815–1818.

Reilinger, R., et al., 2006. GPS constraints on continental deformation in the Africa–Arabia–Eurasia continental collision zone and implications for the dynamics of plate interactions. Journal of Geophysical Research, Solid Earth 111 (B5).

Savage, J., Burford, R., 1973. Geodetic determination of relative plate motion in Central California. Journal of Geophysical Research 95, 4873–4879.

Sengör, A.M.C., 1990. A new model for the late Paleozoic–Mesozoic tectonic evolution of Iran and implications for Oman. The Geology and Tectonics of the Oman region: Geol. Soc. Spec. Publ. London, pp. 797–831.

Sosson, M., et al., 2010. Subductions, obduction and collision in the Lesser Caucasus (Armenia, Azerbaijan, Georgia), new insights. In: Sosson, M., Kaymakci, N., Stephenson, R., Bergerat, F., Starostenko, V. (Eds.), Sedimentary Basin Tectonics from the Black Sea and Caucasus to the Arabian Platform: Geol. Soc. of London.

Stein, S., Gordon, R.G., 1984. Statistical tests of additional plate boundaries from plate motion inversions. Earth and Planetary Science Letters 69, 401–412.

Taymaz, T., Eyidogan, H., Jackson, J., 1991. Source parameters of large earthquakes in the East Anatolian fault zone (Turkey). Geophysical Journal International 106, 537–550.

Trifonov, V.G., Karakhanian, A.S., Kozhurin, A.J., 1994. Active faults of the collision area between the Arabian and the Eurasian plates. Proc. of the Conference on Continental Collision Zone Earthquakes and Seismic Hazard Reduction, Yerevan, pp. 56–79.

Vernant, P., Chery, J., 2006. Low fault friction in Iran implies localized deformation for the Arabia–Eurasia collision zone. Earth and Planetary Science Letters 246 (3–4), 197–206.

Vernant, P., et al., 2004. Present-day crustal deformation and plate kinematics in the Middle East constrained by GPS measurements in Iran and northern Oman. Geophysical Journal International 157 (1), 381–398.